Available online at www.sciencedirect.com

ScienceDirect

Mendeleev Commun., 2023, **33**, 661–665

Mendeleev Communications

The lifetime of polychlorophenyl radicals in methanol: a SCC–DFTB molecular dynamics study

Tatyana I. Gorbunova,[a] Natalia S. Kozhevnikova*[b] and Andrey N. Enyashin[b]

[a] *I. Ya. Postovsky Institute of Organic Synthesis, Ural Branch of the Russian Academy of Sciences, 620108 Ekaterinburg, Russian Federation*

[b] *Institute of Solid State Chemistry, Ural Branch of the Russian Academy of Sciences, 620990 Ekaterinburg, Russian Federation. E-mail: kozhevnikova@ihim.uran.ru*

DOI: 10.1016/j.mencom.2023.09.023

The state of molecules of mono-, di-, and trichlorobenzenes in the gas phase and methanol solution is explored using quantum chemical molecular dynamics simulations. It is proved that saturation of chloroaryl radicals in methanol is realized using a hydrogen atom from the methyl group of solvents rather than from the hydroxyl group in most cases. No evident correlation was established between the lifetimes and other properties of radicals or their parent molecules, pointing to the importance of a solvate shell as a factor controlling the migration and diffusion of H atoms during the saturation of chloroaryl radicals.

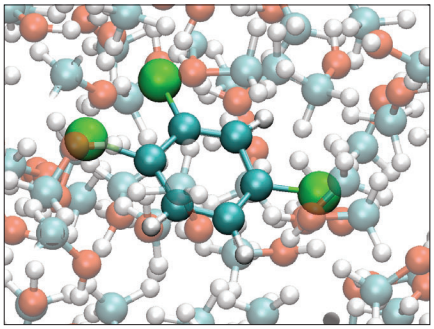

Keywords: quantum chemical modeling, polychlorobenzenes, radicals, bond energy, lifetime.

Polychlorobenzenes serve as important solvents and precursors in chemical manufacturing for industrial applications and agricultural production. The wide use and relatively high inertness of polychlorobenzenes as aromatic systems have led to their progressing accumulation in natural environment and pollution of air, soil, plants, groundwaters and coastal sediments.[1–6] Aside from their own hazard, polychlorobenzenes, being inevitably exposed to sunlight irradiation, can undergo a slow degradation in biosubstrates, under both aerobic and anaerobic conditions, into other compounds unwelcomed by biosphere. In this sense, 1,2,4-trichlorobenzene is the most remarkable representative of the polychlorobenzene family. The half-life of this chloroorganic contaminant produced annually in amount of several thousand tons varies between 128 and 1284 h (5–53 days) under photooxidation in air.[7] It is one of the 188 chemicals recognized as the hazardous air pollutants under the US Clean Air Act[8] and it is blacklisted by the US National Primary Drinking Water Regulations.[9] Accumulation of polychlorobenzenes as well as their decay products in living organisms can provoke misregulation of homeostasis, depression of immune system and carcinogenesis.[10–12]

The destiny of different chloroaromatic compounds in natural environment is governed in many aspects by the strength of covalent C–Cl bond, since the main paths of their destruction *via* photodecomposition and oxidation involve formation of aryl radicals and chlorine atoms as intermediates.[13,14] A controllable transformation of wasted polychlorobenzenes and related polychlorobiphenyls into usable or environmentally safe compounds is also proposed to involve dissociation of the C–Cl bond on the basis of chemically, thermochemically, electrochemically or radiolytically stimulated reactions.[15–21] While the exact scenario of the C–Cl cleavage within polychlorobenzenes can be essentially different or yet debatable for a particular process (radicalization, ionization, preliminary fission of HCl, substitution, *etc.*), the energy of C–Cl bond dissociation remains the fundamentally important parameter for analyses of both molecular stability and ascertainment of the degradation paths of polychlorobenzenes. Therefore, a great effort has been undertaken for accurate theoretical description of bond dissociation energies within polychlorobenzenes or their derivatives to complement scarce experimental data.[22–25]

Despite the modern progress in computational facilities, the high-level *ab initio* calculations of polychlorobenzenes as for many other organic molecules rely on information about the state of an individual molecule (*i.e.* an extremely rarefied gas phase at 0 K). Though, a more practical interest evolves regarding the states of molecules closely resembling their genuine surrounding in a solution or on a surface. In the present work, we employ a tight-binding approach of the density functional theory method for molecular dynamics simulations of mono-, di- and trichlorobenzenes (MCB, DCB and TCB, respectively) in different media.[†] After

[†] *Computational aspects.*

All the molecular dynamics (MD) simulations were carried out using the self-consistent charge density functional tight-binding (SCC–DFTB) method[26,27] in conjunction with universal force field (UFF) method[28] for a correct description of intermolecular dispersion interactions as implemented in deMon 1.1 program.[29,30] The 3OB parametrization set[31,32] of Slater–Koster parameters developed for covalently bound biological and organic systems was employed throughout all the simulations. The family of chloroaromatic species was represented by monochlorobenzene (MCB), 1,2-, 1,3- and 1,4-dichlorobenzenes (DCBs), and 1,2,3-, 1,2,4- and 1,3,5-trichlorobenzenes (TCBs).

At the first stage, the C–Cl bond dissociation energies in the gas phase and in the methanol solution were determined using SCC–DFTB/UFF method. The methanol solution was simulated as a periodic cubic supercell,

validation of the chosen scheme by comparison with available theoretical and experimental data on C–Cl bond dissociation energies in the gas phase, the C–Cl bond dissociation and the lifetimes of the forming aryl radicals are investigated for molecules dissolved in methanol as an universal solvent. The proposed calculational scheme can become a useful tool in behavioral study of other chloroaromatic molecules embedded in a medium.

Typical profiles of the total energy curves of both singlet and triplet states of polychlorobenzene molecules in the gas phase are displayed in Figure 1 for MCB as an example. The singlet state of MCB is the ground state with a deep single energy minimum at an equilibrium C–Cl distance of ~1.75 Å. All conformers of singlet MCB during MD simulation preserve its planar configuration with the Cl atom placed in the plane of the benzene ring. In contrast, the total energy curve for MCB in the triplet state does not possess a well-defined minimum and is plateau-like in shape in a wide range of C–Cl distance values. Conformations of triplet MCB demonstrate a notable distortion of the benzene ring with the C–Cl fragment pointing out-of-plane of the former benzene ring (see insets in Figure 1).

The obtained total energy functions allow estimation of the C–Cl bond dissociation energy (BDE) required for the formation of a (chloro)phenyl radical. The BDE was calculated as the difference between the energy of the triplet state with a C–Cl distance of 3 Å and the energy of the singlet state with an equilibrium C–Cl distance. The BDE values found for all the explored chloroarenes fall in the range of 83.5–93.3 kcal mol^{-1} and are listed in Table 1 alongside with the available experimental, thermochemically derived or quantum-chemical data.

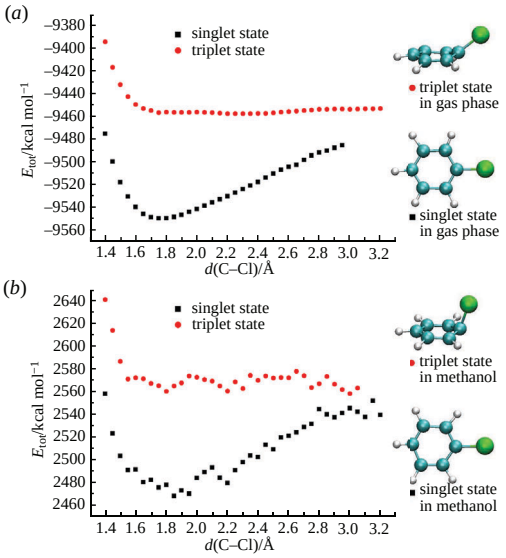

Figure 1 Total energy curves for the supercells containing a single molecule of MCB (*a*) in the gas phase and (*b*) in the methanol solution. The data for singlet and triplet states are plotted using black and red dots, respectively. The insets depict a typical conformation of molecule at the corresponding equilibrium C–Cl distance. For clarity, methanol molecules are not rendered. SCC–DFTB/UFF MD simulations were performed as for the NVT ensemble at T = 300 K.

Noticeably, the predictive power of molecular dynamics using SCC–DFTB method does not concede that of the more sophisticated quantum-chemical methods. Yet it does not employ any approximation of the temperature factor and accounts for energies averaged statistically over an ensemble of thermally

Table 1 The C–Cl bond dissociation energy (BDE) for individual molecules of mono-, di- and trichlorobenzenes obtained in the present MD SCC–DFTB simulation at T = 300 K compared with the available experimental or thermochemical data and with the data obtained by the former high-level DFT and CCSD calculations extrapolated to T = 298 K.

Molecule	Bond	BDE/kcal mol^{-1}					
		Exp.[34]	SCC–DFTB (MD 300 K) (this work)	CCSD(T,Full) (298 K)[22]	DFT B3P86 (298 K)[23]	DFT B3LYP (298 K)[24]	DFT BLYP (0 K)[25]
MCB	C–Cl(1)	95.1[a]	93.27	97.33	94.13	89.46	88.18
1,2-DCB	C–Cl(1)	92.2	88.99	97.45	92.71	87.57	86.06
1,3-DCB	C–Cl(1)	89.9	92.36	97.14	93.39	88.65	87.30
1,4-DCB	C–Cl(1)	93.7	87.21	97.76	94.16	89.40	88.24
1,3,5-TCB	C–Cl(1)	94.5	92.25	96.95	92.72	87.92	86.50
1,2,3-TCB	C–Cl(1)	-	86.19	96.95	-	86.36	84.75
	C–Cl(2)	-	87.35	97.69	-	85.84	84.16
1,2,4-TCB	C–Cl(1)	-	84.08	97.97	-	87.70	86.33
	C–Cl(2)	-	83.50	97.40	-	87.03	85.50
	C–Cl(4)	-	83.55	97.54	-	88.74	87.51

[a] 94.5 (thermochem.)[35], 94 (thermochem.).[36]

spanning on 30 Å in all three directions and containing 402 methanol molecules (2412 atoms) and a single chloroarene molecule (12 atoms). The volume of the supercell was chosen as the sum of experimentally tabulated molecular volumes of individual components. All intra- and intermolecular interactions within the solvent were treated using UFF method. UFF was employed as well for description of intermolecular interactions between chloroarene and solvent molecules, hence, realizing QM/MM coupling. The atom charge formula of methanol corresponded to $C^{-0.292}H^{+0.189}{}_3O^{-0.657}H^{+0.382}$. Dissociation of the C–Cl bond was reproduced as a set of consecutive MD simulations at a fixed bond length, varying from 1.4 to 3.0 Å with a step of 0.05 Å. Every but the first MD simulation was performed as for the NVT ensemble during 1 ps with a time step of 0.5 fs and using the global Berendsen thermostat[33] with the time constant 100 fs at temperature T = 300 K. The first (initial) MD simulation included preliminary thermalisation during 5 ps under the same MD conditions. The total energy curves for singlet and triplet states of a chloroarene molecule were plotted after statistical averaging of the total energies of all supercell conformers appearing on the equilibrium MD trajectory.

At the second stage, the lifetime of a chlorarene radical in the methanol solution was estimated. Here, the full quantum-chemical SCC–DFTB description of solution was employed. The model was represented as a periodic cubic supercell with the lattice parameter 11.16 Å, containing 18 methanol molecules together with a chlorarene species, *i.e.* radical or molecule (119 or 120 atoms in total). Preliminary, every model solution of molecular chlorarene in the singlet state was thermalised as the NVT ensemble during 10 ps with a time step of 0.5 fs and using the global Berendsen thermostat with the time constant 100 fs at T = 300 K. Afterwards, a single Cl atom was deleted, forming a desired radical in a doublet state. Then, the solution was annealed under the same MD conditions with the smaller time step 0.1 fs until capture of a hydrogen atom from the methanol medium. Dynamic stability of the new C–H bond was confirmed by further MD simulation continued for 0.2 ps.

excited conformations. Both experimental and calculated data do not permit to conclude on a clear pattern of the BDE as a function of the type of polychlorobenzene. In general, the heavier chlorination of the benzene ring, the lower the BDE for the first homolytic dissociation. In contrast to other DFT studies, our data hint that homolytic C–Cl dissociation of *meta*-substituted 1,3-dichloro- and 1,3,5-trichlorobenzene may require a slightly larger energy, comparable to that for MCB. Probably, initiation of their dissociation would require more harsh conditions, than in the case of *ortho*- and *para*-substituted chlorobenzenes.

Successful operation of the chosen calculational scheme in sufficiently accurate quantitative description of homolytic C–Cl cleavage in the gas phase enables its extension on dissolved chlorobenzenes.† Methanol was chosen as a model solvent, since it contains both hydrophobic and hydrophilic groups reproducing a natural environment like humus or biological medium. In addition, methanol is considered as a perspective medium and sacrificing agent for catalytic photodestruction of chloroarenes under UV irradiation.[37,38]

The total energy curves for the exemplary case of the MCB molecule in singlet and triplet states in methanol are plotted in Figure 1. The general profiles of the curves resemble those for molecules in the gas phase, yet a noise and new local minima become apparent due to both thermally induced reorganization of the methanol structure and interactions of the solute with labile solvent molecules. Therefore, the curves were approximated using 6-order polynomials for further analysis. According to calculations of solvation energies, solvation of all polychlorobenzenes in methanol is exothermic and gets stronger with the number of chlorine atoms and their mutual remoteness, *i.e.* with the molecular surface area available for interaction with solvent (Table 2).

In the case of the triplet state of a (poly)chlorobenzene molecule, the amplitude of energy noise exceeds the shallow minima of energy, if exist. The rise of new local minima on the energy curve for the singlet (ground) state may be related to the cage effect of the solvent and to existence of one or several stable configurations of solvates. Interaction of the MCB molecule with a methanol medium causes an elongation of the C–Cl bond by ~0.1 Å and an increase in BDE by ~0.8 kcal mol^{-1}, compared to those in an isolated MCB molecule. Similar profiles of the total energy curves can be observed for other polychlorobenzenes. For majority of compounds the BDE values become higher by 0.6–12.5 kcal mol^{-1} due to solvation; hence, the solvate shell obstructs C–Cl dissociation and migration of the Cl atom into solution (Table 2). The only *meta*-substituted 1,3-dichloro- and 1,3,5-trichlorobenzenes demonstrate the opposite trend,

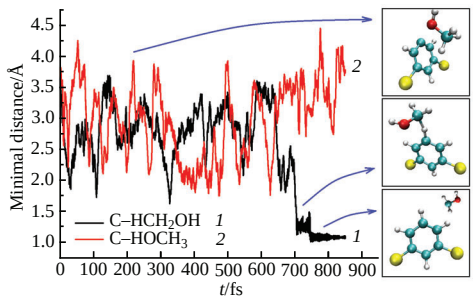

Figure 2 Least distance between the unsaturated C atom in the 3,5-$Cl_2C_6H_3$·(1) radical (1,3,5-TCB with Cl atom eliminated from position 1) and the H atoms in (*1*) methyl and (*2*) hydroxyl groups in methanol. The insets from top to bottom show the structures at notable times corresponding to the existence of the initial radical in the methanol solution, to the rise of the C–H–C transition complex between a radical and a methanol molecule and to the appearance of final products: 1,3-DCB molecule and hydroxymethyl radical. For clarity, unreacting methanol molecules are not depicted. SCC–DFTB MD simulations were performed as for the NVT ensemble at T = 300 K.

Table 2 The C–Cl bond dissociation (BDE) and solvation (ΔH_{solv}) energies for molecules of mono-, di- and trichlorobenzenes in methanol at T = 300 K. The confidence interval does not exceed ±3 kcal mol^{-1}. SCC–DFTB/UFF MD simulations were performed as for the NVT ensemble.

Molecule	Bond	BDE/kcal mol^{-1}	ΔH_{solv}/kcal mol^{-1}
MCB	C–Cl(1)	94.1	−18.9
1,2-DCB	C–Cl(1)	93.5	−19.6
1,3-DCB	C–Cl(1)	82.8	−20.5
1,4-DCB	C–Cl(1)	91.6	−24.7
1,3,5-TCB	C–Cl(1)	90.4	−21.7
1,2,3-TCB	C–Cl(1)	94.8	−25.7
	C–Cl(2)	94.8	
1,2,4-TCB	C–Cl(1)	87.2	−25.0
	C–Cl(2)	84.1	
	C–Cl(4)	96.0	

possessing the BDEs lower by 9.6 and 1.9 kcal mol^{-1}, respectively.

MD simulations of polychlorobenzenes in the triplet state did not unveil their spontaneous dissociation in the methanol solution during 0.1 ns, which can be accepted as the lower bound for their lifetime. Employment of MD simulations also permits a direct estimation of lifetime of forming a chloroaryl radical as the time period required for the aryl radical to capture an atom from solvent and, consequently, to saturate. This scheme does not require any preliminary assumption on the molecular structure and vibrational modes of the transition state as well as accounts the influence of solvent as a statistical ensemble of particles at a given temperature. Saturation of chloroaryl radicals in methanol is possible *via* two paths of H atom capture: from either methyl or hydroxyl groups, forming hydroxymethyl ·CH_2OH or methoxy radical ·OCH_3, respectively. All available conjectures on the reaction products give preference to the formation of ·CH_2OH and they are based mostly on the lower formation energy of ·CH_2OH compared to that of ·OCH_3 in the gas phase.[38]

The lifetime of a (chloro)aryl radical can be traced quantitatively using MD trajectory by analysis of the least distance between the unsaturated carbon atom and hydrogen atoms either in methyl or in hydroxyl groups of methanol molecules. A typical time evolution of these least C–H interatomic distances is displayed for the case of the 3,5-$Cl_2C_6H_3$·(1) radical (*i.e.* 1,3,5-TCB with the Cl atom eliminated from position 1) (Figure 2). Initially, H atoms are located at minimal distances about ~2.5–3 Å from the unsaturated C atom, which corresponds to the van der Waals distances. With the launch of MD simulation, these distances oscillate over time between 1.7 and 4 Å, reflecting approach and divergence of different methanol molecules to the unsaturated C atom as well as molecular internal rotation of methyl and hydroxyl groups since these processes are also characterized by a change in the distances to the unsaturated C atom. This competition between the H atoms of methyl and hydroxyl groups is observed until the time of ~710 fs. Afterwards, a sharp drop in the least interatomic distance between some H-atom of methyl groups and the unsaturated C atom proceeds, evidencing capture and formation of the apparently covalent C–C bond with the length of ~1.1 Å. Simultaneously, an increase in the least interatomic distance between the carbon atom under consideration and the H atoms of hydroxyl groups is observed, which corresponds to the values characteristic of the van der Waals distance between the carbon atom within the new C–H group of the benzene ring and the hydroxyl H atom. Such a process was found for almost all the investigated radicals, except for two of them. In most cases, the reaction path includes the

C–H–C transition state observed usually in the period of ~10–40 fs [maximum is 170 fs for 2,3-$Cl_2C_6H_3$·(1) radical], and it ends by the formation of a saturated aromatic ring and a hydroxymethyl radical ·CH_2OH. The exceptions were found for the 3-ClC_6H_4·(1) radical (*i.e.* 1,3-DCB with the Cl atom eliminated from position 1) and 1,2-$Cl_2C_6H_3$·(4) (*i.e.* 1,2,4-TCB with Cl atom eliminated from position 4). The 2,3-$Cl_2C_6H_3$·(1) radical gets saturated using the H atom of a hydroxyl group, giving rise to the methoxy radical ·OCH_3, *i.e.* the reaction path includes the C–H–O transition state. In the case of the the 1,2-$Cl_2C_6H_3$·(4) radical, neither transition state nor final reaction stage have been observed during 5000 fs. Likely, this behavior is related to the stable solvate shell – an extended network of methanol molecules bound *via* hydrogen bonds, forming around the radical.

The lifetimes of all the explored polychlorophenyl radicals in the methanol solution rarely exceed 500 fs (Table 3). Their mutual comparison as well as search for a correlation with BDE values of the corresponding C–Cl bonds or with the solvation energies of parent molecules do not unveil a consistent pattern. Keeping in mind the dynamic nature of the environment and the observation of the long-lived 1,2-$Cl_2C_6H_3$·(4) radical, the main regulation of the lifetime of polychlorophenyl radicals should be more likely related to structure and rigidity of the solvate shell rather than to the characteristics of intra- and intermolecular interactions involving chlorinated aromatic molecules.

Thus, the molecular and radicalized lower polychlorobenzenes have been investigated both in the gas phase and in the methanol solution using quantum chemical molecular dynamics simulations at room temperature. The solvent was modeled either at the hybrid SCC–DFTB/UFF level or using the fully quantum-chemical SCC–DFTB description. Simulations of polychlorobenzenes in the gas phase yield the results that are comparable to the available experiments and to the data from the more sophisticated DFT schemes, while the simulations directly in an environment like methanol are performed for the first time.

The results on C–Cl bond dissociation energies and on radical saturation observed for polychlorobenzenes in methanol suggest that the mechanisms governing the stability of molecules and radicals in natural environment should not be proposed solely on the basis of the data obtained for the gas phase and should account for a different construction of the solvate shell around different (even isomeric) polychlorobenzenes. Typically, the C–Cl bond dissociation consumes a higher energy in methanol, than in the gas phase, yet in a different degree depending on the number of Cl atoms and their mutual remoteness within the molecule. The direct life simulation of polychlorophenyl radicals in methanol unveils that possible deviations from well-accepted mechanisms of their saturation can be more spread. Namely, the reaction of the 3-ClC_6H_4·(1) radical with a methanol medium has yielded a less stable methoxy radical ·OCH_3 instead of the expected hydroxymethyl radical ·CH_2OH. An anomalously long lifetime of the 1,2-$Cl_2C_6H_3$·(4) radical has been registered, which does correlate with the so far inexplicable half-life of hazardous 1,2,4-trichlorobenzene in natural environment being the longest one among other chlorobenzenes. The absence of a precise correlation between the lifetimes and the thermodynamic properties of polychlorophenyl radicals additionally underlines that involvement of the solvate shell should not be ruled out in determination of environmental distribution of chloroaryl radicals.

Table 3 Approximate lifetimes (*t*) of radicals of mono-, di- and trichlorobenzenes in methanol at T = 300 K until the radical captures a hydrogen atom from the solvent, forming the covalent C–C bond. The SCC–DFTB MD simulations were performed as for the NVT ensemble.

Radical	*t*/fs	Radical	*t*/fs
C_6H_5·(1)	120	2,3-$Cl_2C_6H_3$·(1)	430
		1,3-$Cl_2C_6H_3$·(2)	120
2-ClC_6H_4·(1)	340		
3-ClC_6H_4·(1)	160	1,2-$Cl_2C_6H_3$·(4)	>5000
4-ClC_6H_4·(1)	120	1,4-$Cl_2C_6H_3$·(2)	210
		2,4-$Cl_2C_6H_3$·(1)	130
3,5-$Cl_2C_6H_3$·(1)	710		

The work of T.I.G. was performed within the state assignment AAAA-A19-119012290113-8. The work of N.S.K. and A.N.E. was performed within the state assignment AAAA-A19-119031890025-9.

References

1 J. L. Barber, A. J. Sweetman, D. van Wijk and K. C. Jones, *Sci. Total Environ.*, 2005, **349**, 1.
2 J. Zhang, W. Zhao, J. Pan, L. Qiu and Y. Zhu, *Environ. Int.*, 2005, **31**, 855.
3 W. H. Dong, P. Zhang, X. Y. Lin, Y. Zhang and A. Tabouré, *Sci. Total Environ.*, 2015, **505**, 216.
4 H. Wang, J. Hwang, J. Huang, Y. Xu, G. Yu, W. Li, K. Zhang, K. Liu, Z. Cao, X. Ma, Z. Wei and Q. Wang, *Chemosphere*, 2017, **168**, 333.
5 S. Yao, J. Huang, H. Zhou, C. Cao, T. Ai, H. Xing and J. Sun, *Int. J. Environ. Res. Public Health*, 2022, **19**, 13171.
6 I. J. Allan, B. Vrana, J. de Weert, A. Kringstad, A. Ruus, G. Christensen, P. Terentjev and N. W. Green, *Sci. Rep.*, 2021, **11**, 11231.
7 D. van Wijk, E. Cohet, A. Gard, N. Caspers, C. van Ginkel, R. Thompson, C. de Rooij, V. Garny and A. Lecloux, *Chemosphere*, 2006, **62**, 1294.
8 *National Primary Drinking Water Regulations*, United States Environmental Protection Agency, 2023, www.epa.gov.
9 *Toxicological Profiles*, Agency for Toxic Substances and Disease Registry, 2023, www.atsdr.cdc.gov.
10 K. Sepp, A. M. Laszlo, Z. Molnar, A. Serester, T. Alapi, M. Galfi, Z. Valkusz and M. Radacs, *Int. J. Endocrinol.*, 2018, **2018**, 7493418.
11 P.-K. Hsiao, Y.-C. Lin, T.-S. Shih and Y.-M. Chiung, *Int. Arch. Occup. Environ. Health*, 2009, **82**, 1077.
12 S. Aiso, T. Takeuchi, H. Arito, K. Nagano, S. Yamomoto and T. Matsushima, *J. Vet. Med. Sci.*, 2005, **67**, 1019.
13 B. J. Finlayson-Pitts and J. N. Pitts, Jr., *Chemistry of the Upper and Lower Atmosphere: Theory, Experiments, and Applications*, Academic Press, New York, 1999.
14 J. S. Francisco and M. M. Maricq, *Adv. Photochem.*, 1995, **20**, 79.
15 A. A. Vasil'ev, A. S. Burukin, G. M. Zhdankina and S. G. Zlotin, *Mendeleev Commun.*, 2021, **31**, 400.
16 A. V. Maiorova, T. V. Kulikova, T. I. Gorbunova, M. G. Pervova, K. Yu. Shunyaev and L. I. Leontiev, *Dokl. Chem.*, 2020, **495**, 186 (*Dokl. Ross. Akad. Nauk. Khim., Nauki Mater.*, 2020, **495**, 30).
17 N. Vin, F. Battin-Leclerc, H. Le Gall, N. Sebbar, H. Bockhorn, D. Trimis and O. Herbinet, *Proc. Combust. Inst.*, 2019, **37**, 399.
18 N. Wei, D. Xu, B. Hao, S. Guo, Y. Guo and S. Wang, *Water Res.*, 2021, **190**, 116634.
19 A. Ouni, N. Rabaaoui, L. Mechi, N. Enaceur, A. K. D. AlSukabi, E. M. Azzam, K. M. Alenezi and Y. Moussaoui, *J. Saudi Chem. Soc.*, 2021, **25**, 101326.
20 A. A. Jalil, N. F. A. Panjang, S. Akhbar, M. Sundang, N. Tajuddin and S. Triwahyono, *J. Hazard. Mater.*, 2007, **148**, 1.
21 G. Albarrán and E. Mendoza, *Environ. Sci. Pollut. Res.*, 2019, **26**, 17055.
22 L. Wang and A. Tang, *Int. J. Chem. Kinet.*, 2011, **43**, 62.
23 X.-H. Li, Z.-X. Tang and X.-Z. Zhang, *J. Struct. Chem.*, 2009, **50**, 34.
24 T. Watanabe, Z.-Y. Wang, O. Takahashi, K. Morihashi and O. Kikuchi, *J. Mol. Struct.: THEOCHEM*, 2004, **682**, 63.
25 J. Cioslowski, G. Liu and D. Moncrieff, *J. Phys. Chem. A*, 1997, **101**, 957.
26 Th. Frauenheim, G. Seifert, M. Elsterner, Z. Hajnal, G. Jungnickel, D. Porezag, S. Suhai and R. Scholz, *Phys. Status Solidi B*, 2000, **217**, 41.
27 A. F. Oliveira, G. Seifert, T. Heine and H. A. Duarte, *J. Braz. Chem. Soc.*, 2009, **20**, 1193.
28 A. K. Rappe, C. J. Casewit, K. S. Colwell, W. A. Goddard, III and W. M. Skiff, *J. Am. Chem. Soc.*, 1992, **114**, 10024.
29 L. Zhechkov, T. Heine, S. Patchkovskii, G. Seifert and H. A. Duarte, *J. Chem. Theory Comput.*, 2005, **1**, 841.
30 A. M. Köster, R. Flores, G. Geudtner, A. Goursot, T. Heine, S. Patchkovskii, J. U. Reveles, A. Vela and D. Salahub, *deMon, Version 1.2*, NRC, Ottawa, 2004.

31 M. Gaus, A. Goez and M. Elstner, *J. Chem. Theory Comput.*, 2013, **9**, 338.
32 M. Kubillus, T. Kubař, M. Gaus, J. Řezáč and M. Elstner, *J. Chem. Theory Comput.*, 2015, **11**, 332.
33 H. J. C. Berendsen, J. P. M. Postma, W. F. van Gusteren, A. DiNola and J. R. Haak, *J. Chem. Phys.*, 1984, **81**, 3684.
34 E. C. M. Chen, K. Albyn, L. Dussack and W. E. Wentworth, *J. Phys. Chem.*, 1989, **93**, 6827.
35 K. W. Egger and A. T. Cocks, *Helv. Chim. Acta*, 1973, **56**, 1516.
36 K. Y. Choo, D. M. Golden and S. W. Benson, *Int. J. Chem. Kinet.*, 1975, **7**, 713.
37 N. S. Kozhevnikova, T. I. Gorbunova, A. S. Vorokh, M. G. Pervova, A. Ya. Zapevalov, V. I. Saloutin and O. N. Chupakhin, *Sustainable Chem. Pharm.*, 2019, **11**, 1.
38 G. S. Zakharova, N. V. Podval'naya, T. I. Gorbunova, M. G. Pervova, A. M. Murzakaev and A. N. Enyashin, *J. Alloys Compd.*, 2023, **938**, 168620.

Received: 20th April 2023; Com. 23/7153